Analytical Methods

ROYAL SOCIETY OF CHEMISTRY

PAPER

Published on 21 August 2026
Licensed under CC-BY 4.0

Check for updates

Cite this: DOI: 10.1039/d6ay01076h

A combined multivariate approach for the analysis of organic residues in Faliscan figured vases

Adele Bosi, *[a] Martina Negozio,[b] Claudia Frasca,[c] Angela Pola,[d] Federico Marini,[c] Alessandro Ciccola,[e] Gabriele Favero[e] and Ilaria Serafini[e]

Organic residue analysis in biomolecular archaeology provides critical insights into past human practices. However, its application is often hindered by analytical challenges. Traditional single-biomarker approaches are highly susceptible to interference issues, such as contamination and matrix effects. These challenges are exacerbated in high-value artifacts, such as figured vases, which frequently undergo post-excavation washing, restoration, and strict sampling restrictions, thereby demanding highly sensitive and interference-robust methods. To address this, we propose a multivariate analytical framework based on the simultaneous profiling of 12 corroborated molecular markers, including wine acids and fatty acids. This strategy was applied to investigate funerary figured vases from Falerii Veteres (central Italy), targeting residues associated with ritual symposia, where wine was historically blended with honey and dairy products. Crucially, the multivariate approach was utilized not only for data interpretation but also for analytical optimization *via* experimental design. Maximizing the geometric mean of the chromatographic peak areas obtained *via* high-performance liquid chromatography coupled with high-resolution mass spectrometry enabled the simultaneous optimization of the analytical response across all 12 target analytes. Principal component analysis of the archaeological vessels and modern mock-up references demonstrated that this multi-biomarker framework successfully mitigates single-marker vulnerabilities, effectively discriminating between substance classes by leveraging chemical patterns across the entire analyte suite.

Received 1st June 2026
Accepted 4th August 2026

DOI: 10.1039/d6ay01076h

rsc.li/methods

Introduction

State of the art

In biomolecular archaeology, organic residue analysis (ORA) provides a unique window into past civilizations, enabling researchers to address questions related to the ritual, medical, and dietary use of substances,[1–15] the function and intended use of specific ceramic productions,[16,17] and artistic productions in general,[18] as well as patterns of exchange and changes in subsistence strategies following major climatic events or large-scale migrations.[19] However, this field poses substantial analytical challenges, as not all substances leave residues that are readily detectable or identifiable in archaeological contexts.[20–22] ORA methods rarely provide a detailed characterization of the natural origin of ancient products and often struggle to adequately resolve complex mixtures. Analysis of stable carbon isotope ratios of palmitic and stearic acids can only distinguish between ruminant and non-ruminant carcass fats, dairy products, and marine or freshwater oils. Proteomic analyses of residues preserved in archaeological ceramics can offer high taxonomic resolution, but protein preservation occurs only under highly specific conditions.[3] When acyl lipids are preserved, analysis of triacylglycerol profiles can be performed for comparison with those of modern reference materials,[23] but triacylglycerols are rarely detectable in ancient organic residues, and degradation processes preferentially affect the most unsaturated and shortest chain triacylglycerols, thereby altering the original lipid signatures.[23] The major challenge lies in plant-derived products, which are rarely detected and are difficult to characterize at a high taxonomic resolution. This is largely because their main molecular constituents are widely distributed across the plant kingdom and are highly susceptible to degradation.[23] Although wine represents a notable exception, there is still limited consensus regarding its detection, and even the specificity of proposed wine biomarkers has been questioned.[24] This is due to the fact that identification of wine residues is largely based on tartaric acid, which is also present in other fruits and can be formed during the chemical alteration of substances released from plastic sampling containers or conservation products used during sample pre-treatment.[24] This susceptibility to

[a]National Research Council-Institute of Complex Systems (CNR-ISC), P. le Aldo Moro 5, Rome, Italy. E-mail: adele.bosi@uniroma1.it
[b]Sapienza University of Rome, Earth Science Dept., P. le Aldo Moro 5, Rome, Italy
[c]Sapienza University of Rome, Chemistry Dept., P. le Aldo Moro 5, Rome, Italy
[d]University of Oxford, Faculty of Classics, St. Giles', Oxford, UK
[e]Sapienza University of Rome, Environmental Biology Dept., P. le Aldo Moro 5, Rome, Italy

contamination is not specific to wine residues and has also been reported for heating markers, which may be generated during sampling procedures involving drilling[25] and cacao residues.[26] In this scientific context, relying on a single biomarker can be risky, and advancing ORA toward a multivariate approach would help to more robustly address the historical questions at the core of the discipline.

In this regard, untargeted approaches aimed at discovering novel and unique molecular markers for the unambiguous identification of archaeological residues are becoming increasingly common.[1,4,6,10,15,18,27–30] These methodologies, primarily used on residues of plant origin, enable the exploration of long-standing archaeological questions previously deemed unanswerable. However, such metabolomics-based approaches face significant challenges, particularly regarding confounding effects and the high proportion of statistically relevant compounds that remain unannotated. In the case of wine, the work of Roullier-Gall developed a regression model based on untargeted MS and NMR analysis to estimate the age of an unknown wine bottle discovered during restoration work at the Saint-Vivant monastery in Burgundy.[30] By comparing wines of different ages, the authors identified approximately 25 000 compounds that were unique to the specific age groups examined, but about 95% were unannotated, reflecting the chemical complexity and scarce knowledge of wine ageing chemistry in the current state of the art.[31]

From this perspective, the present study develops a multivariate approach based on known markers to distinguish potential organic residues in figured pottery. These vases were extensively used in ritual and banquet contexts but have been only marginally investigated by ORA. This limited attention is primarily attributable to the short contact times with contents, fine clay fabrics, and post-excavation conditions, often involving prolonged storage and conservation treatments, which collectively hinder the preservation, identification, and analysis of organic residues on such artifacts. Consequently, particularly robust analytical strategies are required.

The research was conducted within the framework of the Imag-ORA project, which adopts an interdisciplinary approach to investigate the uses and functions of Etruscan-Italic figured pottery in pre-Roman Italy (see Acknowledgements). Building on previous work by Bartolini and co-authors,[16] which addressed the challenge of identifying wine residues in figure-decorated pottery through the simultaneous evaluation of tartaric, fumaric, and malic acids in a ternary plot, the present study develops an approach which explores the discriminatory potential of 12 molecular markers. These markers, comprising wine acids and fatty acids, are employed to distinguish residues derived from three key substances associated with ritual and banquet practices: wine, milk-derived products, and honey. The simultaneous extraction of both compound classes for detection through high-performance liquid chromatography coupled with high-resolution mass spectrometry (HPLC-HRMS), a golden standard in ORA, is optimized using an experimental design approach.

Experimental design is a statistical and methodological framework which aims to organize experimentation in such a way as to obtain the maximum amount of relevant information with the smallest possible number of experiments.[32–34] This approach arises from the limitations of the traditional one-factor-at-a-time (OFAT) method, in which a single factor is varied, while all others are kept constant. OFAT often requires a large number of experiments and may fail to identify the conditions that maximize the response (Fig. 1).

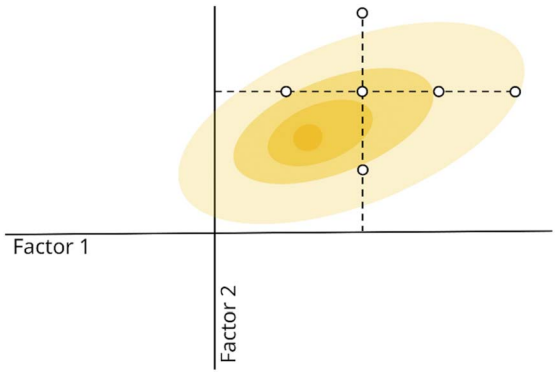

Fig. 1 Schematic illustration of the OVAT (one variable at a time) approach for the optimization of experimental parameters. When two factors (factor 1 and factor 2) are varied individually to reach an apparent optimum response, information on the overall response surface may be entirely lost. Areas of improved response are represented by progressively darker shades of yellow, while the experimental points of the OFAT approach are represented by white markers.

Moreover, this approach does not allow the investigation of interactions between factors, that is, how the effect of one factor on the response changes depending on the level of another factor.

Research rationale

In the present study, experimental factors were optimized for both fatty acids and wine acids by using the geometric mean of the chromatographic peak areas of each compound measured by HPLC-HRMS. The geometric mean emphasized solutions that represent an optimal compromise among all analytes considered. The experimental design encompassed all three stages of the analytical workflow: extraction, derivatization, and clean-up.

Starting from just 35 mg of ceramic powder, strong acidic and basic solutions were selected for ultrasound-assisted liquid extraction, as these have been widely reported in the literature for the recovery of both fatty acids and wine-related organic acids.[16,24,35] Although a milder extraction strategy based on organic solvents (mainly chloroform and methanol, 2 : 1) has been established for lipid substances to avoid hydrolysis of diacylglycerols and triacylglycerols,[36–38] these molecules are rarely detectable in ancient organic residues, as their molecular integrity is often compromised by degradation processes. Consequently, strong acidic or basic solutions at elevated temperatures remain the most effective approach for the extraction of free fatty acids (FFAs) and wine acids from archaeological ceramics, particularly dicarboxylic and hydroxylic acids, which strongly interact with the polar groups of the ceramic.[21,22,35]

 This journal is © The Royal Society of Chemistry 2026

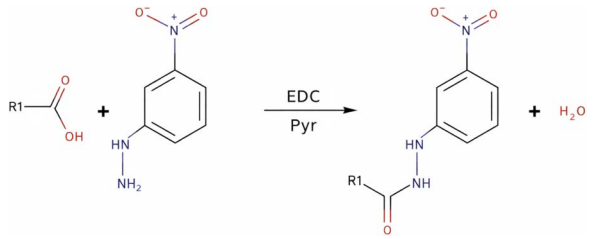

Fig. 2 Derivatization reaction employed to improve analyte separation and detectability. The reaction is carried out in a slightly basic aqueous solution and uses 3-nitrophenylhydrazine (3-NPH) as the derivatizing reagent, leading to the formation of 3-nitrophenylhydrazones. The presence of 1-ethyl-3-(3-dimethylaminopropyl)carbodiimide (EDC) hydrochloride in pyridine activates the carbonyl group, increasing its susceptibility to nucleophilic attack.

Because wine acids are small and highly polar molecules, a derivatization step was required to improve their chromatographic separation and ionization efficiency during HPLC-HRMS analysis. The derivatization procedure employed, first proposed by Han and coauthors[39] and later adopted by other authors,[16,40,41] involves the conversion of carboxylic acids into hydrazones in a slightly basic aqueous solution. This reaction occurs in the presence of 1-ethyl-3-(3-dimethylaminopropyl) carbodiimide (EDC) hydrochloride, a carbodiimide which activates the carbonyl group of carboxylic acids, making it more susceptible to nucleophilic attack by the lone pair of electrons on nitrogen. The reaction, which employs 3-nitrophenylhydrazine (3-NPH) as a derivatizing reagent, follows a nucleophilic addition–elimination mechanism, leading to the formation of 3-nitrophenylhydrazone (Fig. 2).

The clean-up step involved dispersive liquid–liquid microextraction (dLLME), developed within the field of environmental science and successfully applied in several areas of analytical chemistry, including forensic, food, clinical analysis, and cultural heritage.[16,17,42–47] DLLME is highly cost-effective and provides a large contact surface between the analyte and the extracting solvent, thereby enhancing rapid and efficient analyte transfer into the organic phase.

Once optimized and validated, the method was applied to 12 figured vases discovered in Falerii Veteres (now Civita Castellana, Viterbo, Italy), and the results were compared with reference samples specifically prepared and artificially aged under laboratory conditions. Overall, this multivariate method represents a step forward in improving the reliability of ORA in biomolecular archaeology.

Experimental

Materials

Methanol (≥99.9%, Sigma-Aldrich), acetonitrile (≥99.9%, Carlo Erba Reagents), isopropanol (≥99.5%, Sigma-Aldrich), and ethanol (≥99.9%, Carlo Erba Reagents) were all of HPLC grade. Chloroform (≥99.8%) and ethyl acetate (≥99.5%) were purchased from VWR Chemicals and Carlo Erba Reagents, respectively. Formic acid, the derivatization reagents 3-nitrophenylhydrazine (3-NPH) and 1-ethyl-3-(3-dimethylaminopropyl)carbodiimide (EDC) hydrochloride, potassium hydroxide (KOH, ≥85%), sulfuric acid (H_2SO_4, ≥99.9%), hydrochloric acid (HCl, ≥37%), pyridine, and sodium dihydrogen phosphate and disodium hydrogen phosphate salts were purchased from Sigma-Aldrich (Milwaukee, WI, USA). Standards of tartaric, malic, maleic, syringic, fumaric, and succinic acids, as well as standards of butyric, linoleic, myristic, oleic, palmitic, and stearic acids, were also purchased from Sigma-Aldrich. The water used during the procedures was ultrapure water, which was obtained using a Milli-Q Plus Millipore system. Standard solutions of the analytes were prepared at a concentration of 1 mg mL^{-1} in water and acetonitrile (1 : 1) for wine-related organic acids and in ethanol for fatty acids. From these, a mixed standard solution containing all analytes at a concentration of 10 μg mL^{-1} in methanol was prepared. All solutions were stored in a freezer at approximately −20 °C. For the reference materials, the wine was obtained from a local supermarket, and multifloral honey and raw cow milk were obtained from two Italian companies (BeeO Baita and Biolà, respectively).

Analysis

HPLC-HRMS. For chromatographic analysis, a Vanquish Core HPLC system equipped with an autosampler was used. Chromatographic separation of the analytes was carried out on a Phenomenex Kinetex F5 column (2.6 μm, 2.1 × 100 mm). The mobile phases consisted of methanol with 0.1% formic acid (phase A, organic) and water with 0.1% formic acid (phase B, aqueous). The chromatographic gradient was as follows: initial conditions at 30% phase B; phase B increased to 55% in 3 minutes, then to 59% in 6 minutes and to 100% in 7 minutes. Phase B was held at 100% for 2 minutes (until minute 9), then reduced from 100% to 30% at 10.5 minutes and maintained under these conditions until 12 minutes (total run time: 15 minutes). The flow rate was set at 0.25 mL min^{-1}, and the column temperature was kept constant at 35 °C. Mass spectrometric analysis was performed using an Orbitrap Exploris 240 mass spectrometer (Thermo Fisher Scientific), equipped with a heated electrospray ionization (H-ESI) source operating in negative ionization mode. Source parameters were set as follows: H-ESI temperature, 300 °C; transfer tube temperature, 280 °C; spray voltage, 3.2 kV (negative); sheath gas, 30 a.u.; auxiliary gas, 10 a.u. The resolution was set to 120 000, and the scan range was 100–1200 m/z. Structures of the analytes after derivatization, along with their retention times and m/z values, are provided in Table 1.

Optimization. For the optimization of the procedure, an experimental design was adopted for the extraction of the analytes from the ceramic matrix, for the derivatization of the extracted analytes, and for the final clean-up. In all three cases, a full factorial design with four factors at two levels was employed. The overall design of experiments is illustrated in Table 2.

For the extraction optimization, 2 mL of a standard solution containing all the analytes (10 μg mL^{-1}) were poured into a vase

Table 1 Analyte names, structures, chemical formulae, exact mass, molecular ions, fragments and retention times

Name	Structure	Formula	Exact mass (Da)	Molecular ion (m/z)	Fragments (m/z)	Retention time (min)
Butyric acid	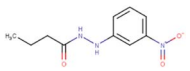	$C_{10}H_{13}N_3O_3$	223.0956	222.0878	185.875 145.930 141.868 137.035	5.20
Linoleic acid	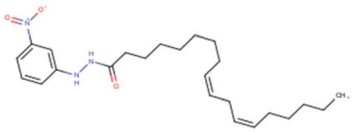	$C_{24}H_{37}N_3O_3$	415.2834	414.2756	249.149 353.248 130.944 152.046	10.82
Myristic acid	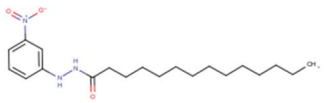	$C_{20}H_{33}N_3O_3$	363.2521	362.2443	107.037 137.035 152.046 319.239	10.65
Oleic acid	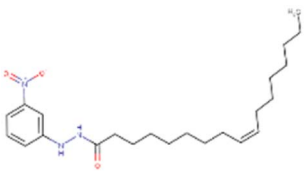	$C_{24}H_{39}N_3O_3$	417.2991	416.2913	390.274 248.960 130.944 398.233	10.95
Palmitic acid	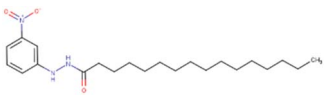	$C_{22}H_{37}N_3O_3$	391.2834	390.2756	322.208 260.850 207.655	10.87
Stearic acid	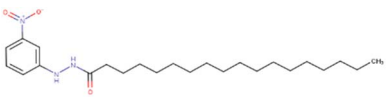	$C_{24}H_{41}N_3O_3$	419.3147	418.3069	137.035 152.046 375.301	11.10
Fumaric acid	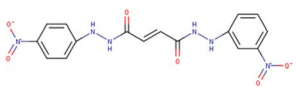	$C_{16}H_{14}N_6O_6$	386.0974	385.0896	122.024 232.036 234.052 96.009	7.19
Maleic acid	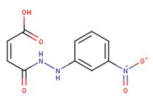	$C_{10}H_9N_3O_5$	251.0542	250.0463	112.985 206.057 222.052 208.036 137.035	8.25
Malic acid	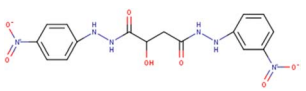	$C_{16}H_{16}N_6O_7$	404.1080	403.1002	207.836 208.036 137.035	5.89
Syringic acid	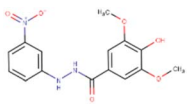	$C_{15}H_{15}N_3O_6$	333.0960	332.0882	166.014 122.024	6.37
Succinic acid	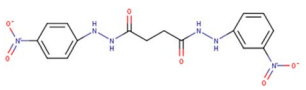	$C_{16}H_{16}N_6O_6$	388.1131	387.1053	234.052 98.024 191.046	6.26
Tartaric acid	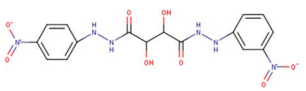	$C_{16}H_{16}N_6O_8$	420.1029	419.0951	208.036 137.035 266.042	5.19

prepared specifically with local clay. Once dry, 35 mg of ceramic material was scraped from the inside of the vase with a sterile scalpel. The resulting scrapings were then homogenized and subjected to extraction according to the experimental design. The four factors considered are the extraction solvent (KOH and H_2SO_4), their concentration (1 M and 0.4 M), the extraction temperature (70 °C and 20 °C), and the extraction time (90 and 30 minutes). The solvents and their concentrations were

This journal is © The Royal Society of Chemistry 2026

Table 2 Design of experiments

	Factor	Level +	Level −
Extraction	Extraction solvent	KOH	H_2SO_4
	Extraction solvent concentration	1 M	0.4 M
	Extraction temperature	70 °C	20 °C
	Extraction time	90 minutes	30 minutes
Derivatization	Time	30 minutes	15 minutes
	Temperature	45 °C	20 °C
	EDC concentration	24 mM	12 mM
	3-NPH concentration	40 mM	20 mM
Clean-up	Extraction solvent	Ethyl acetate	Chloroform
	Disperser solvent	Isopropanol	Acetonitrile
	Disperser/extraction solvent ratio	1 : 1	2 : 1
	NaCl	0.3 g	0.2 g

selected based on two different methods reported in the literature for the extraction of fatty acids and wine acids,[16,24,35] taking into account both the temperatures reported and room temperature.

For the derivatization optimization, the experiments started from 10 microliters of a mixed standard solution at 10 μg mL^{-1}, added into aqueous solution and subjected to the derivatization process. The factors considered are time (30 and 15 minutes), temperature (45 and 20 °C), EDC concentration (24 and 12 mM), and 3-NPH concentration (40 and 20 mM). The factor levels were chosen based on the parameters adopted by Bartolini *et al.*[16] for the extraction of wine acids, as well as parameters that allow savings in time, energy, and reagents where possible, within a sustainable chemistry perspective that does not alter the efficiency of the procedure.

Once the derivatization parameters were defined, the clean-up optimization was carried out similarly, starting from 10 microliters of the mixed standard solution at 10 μg mL^{-1}, which was added in aqueous solution and derivatized. For the clean-up step, dispersive liquid–liquid microextraction was used (dLLME), and the factors considered were extraction solvents (chloroform and ethyl acetate), disperser solvents (isopropanol and acetonitrile), disperser/extraction solvent ratio (1 : 1 and 2 : 1), and NaCl concentration (0.3 and 0.2 g). The response for each experiment in the experimental design was calculated as the geometric mean of the chromatographic peak areas of the 12 analytes, normalized between 0.9 and 0.1, and set to 0.001 in the absence of a chromatographic peak.

Based on the response obtained from each experimental combination, only factors with a *p*-value lower than 5.00% were considered significant. This means that, when a factor was not significant, the probability of obtaining an effect such as the observed one was lower than 5.00%. It was then verified that all assumptions of the applied tests were met. Data normality was assessed using the Shapiro–Wilk test. A *p*-value lower than 5.00% would lead to rejection of the null hypothesis of normal distribution. Homogeneity of variance among groups was evaluated using the non-parametric Fligner–Killeen test. A *p*-value higher than 5.00% indicates that the null hypothesis of equal variances across populations cannot be rejected. After verifying the adequacy of the model, center-point experiments were performed for the non-categorical factors to assess whether the response maximum was located within the center of the investigated experimental domain. Four samples were prepared by fixing the categorical factors at their selected levels and setting the non-categorical factors at the mean values of the original design and subsequently analyzed. If the predicted central point was statistically consistent with the experimental responses (*t*-test *p*-value > 5.00%), the non-categorical factors were further investigated along the direction of steepest ascent until the response maximum was identified. All statistical analyses, calculations, and graphical representations were performed using custom scripts in R (version 4.4.2) within the RStudio environment (version 2024.12.1).

Validation. The proposed method was validated for the target analytes by assessing the following parameters: precision, carryover, and limit of detection (LOD), following the international guidelines. The screening approach is intended to assess the concomitant presence of multiple analytes, to ensure analytical robustness. Precision was evaluated through independent assays performed on four quality control (QC) samples. QC samples were prepared by spiking blank samples with a standard mixture containing the target analytes. Precision was expressed as relative standard deviation (RSD%). Carryover was assessed by analyzing a blank sample immediately after injection of both the highest calibration standard and a real sample. The LOD was defined as the lowest absolute concentration yielding a signal-to-noise (S/N) ratio greater than 3. To determine the LOD, decreasing concentrations of the standard mixture (five points between 50 and 0.5 ng mL^{-1}) were processed using the described method and analyzed across three chromatographic runs. Furthermore, linearity was checked between peak areas (driving the PCA) and the analyte concentration.

Case studies. The vases analyzed in this study were all produced in the first half of the 4th century BC in Ager Faliscus, an important territory of pre-Roman Italy dependent on the city of Falerii Veteres, present-day Civita Castellana, in the province of Viterbo. The full set of vases analyzed, together with their stylistic and conservative characteristics, are summarized in Table 3.

The vases belong to local red-figure, overpainted, and black-gloss productions. All specimens were recovered during excavations carried out between the late 19th and early 20th

Table 3 List and images of the analyzed vases, with provenance and description of stylistic and conservative information

Inv. no.	Vase shape	Decorative technique	Attribution	Condition	Provenance	Vase bibliography	Image
1062	Stamnos	Overpainted	Civita Castellana group	Intact	Falerii Veteres, Valsiarosa, tomb 12 (XCV)	Cozza–Pasqui 1981, p. 196, no. 9 (ref. 48) Pola 2024, p. 39, no. 28, pl. XIV a–c[49]	
1128	Stamnos	Overpainted	Civita Castellana group	Intact	Falerii Veteres, Valsiarosa, tomb 9 (XCVIII)	Cozza–Pasqui 1981, p. 194, no. 4 (ref. 48) Pola 2024, p. 39, no. 29, pl. XV a–c[49]	
1200	Hydria	Red-figure	Painter of the Berkeley Hydria	Intact	Falerii Veteres, Celle, tomb 21 (XCIX)	Cozza–Pasqui 1981, p. 135, no. 10 (ref. 48) Pola 2024, p. 174, no. 5, pl. CCI–CCII[49]	
1219	Oinochoe	Overpainted	Civita Castellana group	Intact	Falerii Veteres, Celle, tomb 21 (XCIX)	Cozza–Pasqui 1981, p. 136, no. 22 (ref. 48)	
1220	Oinochoe	Overpainted	Civita Castellana group	Intact	Falerii Veteres, Celle, tomb 21 (XCIX)	Cozza–Pasqui 1981, p. 136, no. 22 (ref. 48)	
1221	Oinochoe	Overpainted	Civita Castellana group	Intact	Falerii Veteres, Celle, tomb 21 (XCIX)	Cozza–Pasqui 1981, p. 136, no. 21 (ref. 48)	
1229	Oinochoe	Overpainted	—	Intact	Falerii Veteres, Celle, tomb 21 (XCIX)	Cozza–Pasqui 1981, p. 136, no. 23 (ref. 48)	
1556	Askos	Red-figure	—	Intact, except for a chipped spout at the terminal end	Falerii Veteres, Valsiarosa, t. 8 (CXIII)	Cozza–Pasqui 1981, p. 193, no. 2 (ref. 48) Pola 2024, p. 617, no. 21 (ref. 49)	
6208	Stamnos	Red-figure	Nazzano group	Intact	Corchiano, Secondo Sepolcreto del Vallone, t. 15	Cozza–Pasqui 1981, p. 269, h[48] Pola 2024, p. 133, no. 1, pl. CXXV[49]	

This journal is © The Royal Society of Chemistry 2026

Table 3 (*Contd.*)

Inv. no.	Vase shape	Decorative technique	Attribution	Condition	Provenance	Vase bibliography	Image
6279	Oinochoe	Black gloss	Civita Castellana group	Intact	Corchiano, Secondo Sepolcreto di S. Antonio, t. 6	Cozza–Pasqui 1981, p. 300, c[48]	
6451	Stamnos	Black gloss	—	Intact	—	—	
6535	Oinochoe	Red-figure	Fluid group	Intact	Corchiano, Primo Sepolcreto di S. Antonio, t. 20	Cozza–Pasqui 1981, p. 295, b[48]	

centuries (for a history of these excavations: Cozza-Pasqui 1981 (ref. 48) and Pola 2024, pp. 1–6 (ref. 49)) from chamber tombs of the area (necropolis of Civita Castellana, Falerii Veteres, and Corchiano), where they formed part of symposium sets intended to accompany the deceased on their journey to the afterlife. After their discovery, the vases were first housed in the Museo di Villa Giulia in Rome and were later transferred to the Museo dell'Agro Falisco in Civita Castellana, where they have largely been kept in storage. For the present analyses, closed shapes (stamnoi and oinochoai, as well as a chous) were selected, in order to minimize the visible damage due to the sample technique, prioritizing complete specimens that had not undergone restoration interventions. As a reference for the real samples, three fragments of a vase specifically produced by a local artisan from Civita Castellana, specialized in traditional craftsmanship and ancient manufacturing techniques, were used. The vase was produced using locally sourced clay with a composition comparable to that of the archaeological specimens under investigation, and the fragments were, respectively, fortified with 2 mL of white wine, milk, and honey. These substances were selected based on their documented significance in ritual contexts: indeed, historical and archaeological sources indicate that wine could be blended with honey and dairy products during consumption and at symposia, especially in non-Greek cultural contexts. An analogous vase fragment that had not been in contact with any substance was used as the ceramic blank. The purpose of these reference samples was not to literally replicate ancient matrices, but to provide a simplified control model for comparison.

The fragments underwent accelerated thermal ageing using an M410 microoven (F. lli Galli G&P, Milan, Italy) set at 65 °C for 90 hours, followed by UV ageing in a QUV Accelerated Weathering Tester (Q-LAB Europe, Bolton, UK), maintained at a constant temperature of 60 °C with UVB radiation at a wavelength of 313 nm. Rather than replicating centuries of complex degradation, artificial ageing aimed to induce a baseline alteration to verify biomarker survival within the ceramic matrix. Additionally, UV exposure was aimed at mimicking post-excavation ageing, reflecting the conditions typical of museum display environments where these figured vessels are exhibited.

An aliquot of 35 mg of scrapings was obtained by scraping the inner surface of each vase, both the original samples and the laboratory references, with a sterile scalpel. After mixing, the sample was subjected to the optimized extraction, derivatization, and clean-up procedures. Specifically, 35 mg of scraped sample was mixed with 200 μL of 0.4 M KOH and placed in an ultrasonic bath at 20 °C for 30 minutes. After this period, 30 μL of 0.4 M HCl and 35 μL of NaH_2PO_4/Na_2HPO_4 buffer solution were added to adjust the pH to 8. Derivatization of the extract was then carried out by adding 150 μL of 40 mM 3-NPH in water and isopropanol (30 : 70) and 150 μL of 24 mM EDC in water and isopropanol (30 : 70) containing 6% pyridine, and the reaction was allowed to proceed under agitation on a Thermomixer for 15 minutes at 20 °C. After the reaction time, 200 μL of 0.1% formic acid (HCOOH) in water was added to quench the derivatization. Subsequently, the samples were centrifuged at 4500 rpm for 10 minutes, and 1.235 mL of water was added. The

supernatant was transferred into a 15 mL Falcon tube containing 0.426 g of NaCl. For the dispersive dLLME, 200 μL of an extractant–disperser mixture of chloroform and isopropanol (1 : 1) was added. After sonication for 10 minutes at 25 °C and centrifugation at 4500 rpm for 10 minutes, the extract was evaporated to dryness using a Vacuum Concentrator (Thermo Fisher), reconstituted in 100 μL of methanol (MeOH), centrifugated at 4500 rpm for 10 minutes, and the supernatant was transferred into glass vials for the analysis. A method blank was prepared, which underwent the whole sample preparation with no analytes. For each sample, duplicate extractions were performed, and each was analyzed in instrumental duplicate.

Statistical interpretation was carried out *via* Principal Component Analysis (PCA) using the peak areas of the analytes. The analysis included both experimental mock-up samples and archaeological samples to investigate diagnostic clusters. Prior to PCA, data were autoscaled. Analytes with low analytical precision (RSD > 15%) and linearity (R^2 < 0.80) were excluded to improve the signal-to-noise ratio. Venetian blind cross-validation with five groups was employed to select the optimal number of principal components. All the analyses were performed using custom scripts in R (version 4.4.2) within the RStudio environment (version 2024.12.1).

Results and discussion

Optimization

Extraction. Among the extraction parameters tested, only the extraction solvent proved to be statistically significant, with a *p*-value of 0.03%. Specifically, the normalized geometric mean of the chromatographic peak areas of the 12 analytes was higher by 396% following extraction with KOH compared with H_2SO_4 (Fig. 3).

The majority of the analytes investigated showed substantially higher chromatographic peak areas following extraction with KOH. The most marked enhancements were observed for tartaric, succinic, and malic acids, which reached signal intensities on the order of 10^4 in H_2SO_4 and 10^8 in KOH. In contrast, linoleic and maleic acids exhibited comparable responses under both extraction conditions.

Neither the concentration of the extracting solution nor the extraction time and temperature were found to be significant factors for the response under investigation. The Shapiro–Wilk (SW) test for normality yielded a *p*-value of 97.40%, while the Fligner–Killeen test for homogeneity of variance yielded all the *p*-values above 5.00% (Fig. S1 and S2, SI). To verify that the response optimum did not lie at the center of the experimental design, four replicate KOH extractions were performed with extraction temperature and time set at intermediate values relative to those originally considered (45 °C and 60 minutes). The *t*-test showed no statistically significant difference between the value predicted by the model and the four experimental replicates, yielding a *p*-value of 13.42%. It was therefore decided to maintain the KOH concentration at 0.4 M and to perform the extraction at room temperature for 30 minutes.

Derivatization. For the derivatization step, none of the four factors investigated showed a statistically significant effect on the analytical response. The experiment was repeated three times to assess reproducibility. Data normality and homogeneity of variances were confirmed by the SW test and the Fligner–Killeen test, respectively (Fig. S3 and S4, SI). Four replicates of the intermediate experimental point were analyzed to verify that the optimal response did not lie at the centre of the experimental design. The subsequent *t*-test yielded a *p*-value of 42.99%, indicating no statistically significant difference among the conditions examined. Consequently, the derivatization time and temperature were set to 15 minutes and 20 °C, respectively, while the concentrations of 3-NPH and EDC hydrochloride were kept unchanged.

Clean-up. Experiments performed for the dLLME step identified two statistically significant factors: the extraction solvent (*p*-value = 0.16%) and the amount of NaCl (*p*-value = 2.51%). A graphical representation of the effects of these factors is shown in Fig. 4.

Data normality and homogeneity of variances were confirmed by the SW test (*p*-value = 56.00%) and the Fligner–Killeen test (all *p*-values > 5.00%), respectively (Fig. S5 and S6, SI). Since chloroform provided a statistically significant improvement in the analytical response compared to ethyl

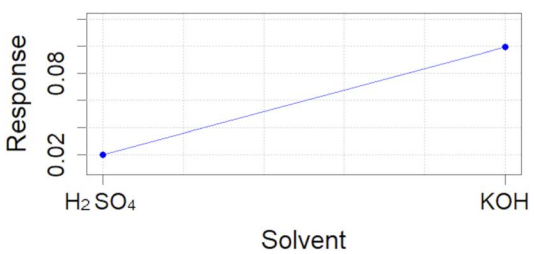

Fig. 3 Impact of the extraction solvent on the geometric mean of chromatographic peak areas for the 12 analytes considered, normalized between 0.1 and 0.9. The effect was statistically significant (*p*-value: 0.03%).

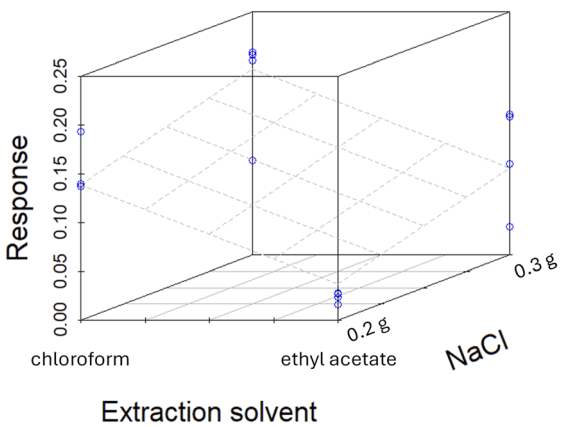

Fig. 4 Impact of the extraction solvent and NaCl on the geometric mean of chromatographic peak areas for the 12 analytes considered, normalized between 0.1 and 0.9. Both the effects resulted to be statistically significant with a *p*-value of 0.15% (solvent) and 2.51% (NaCl).

This journal is © The Royal Society of Chemistry 2026

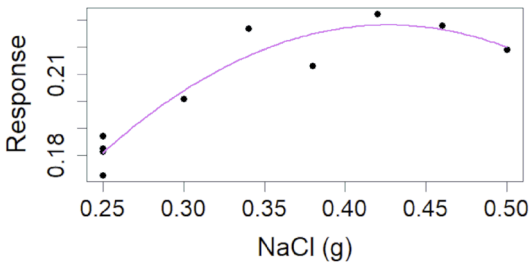

Fig. 5 Effect of NaCl concentration on the analytical response. Experimental data points are shown together with the fitted second-order polynomial model (purple line).

acetate, it was selected as the extraction solvent. Isopropanol was chosen as the disperser solvent over acetonitrile due to its lower toxicity. The central point employing chloroform and isopropanol, with the NaCl concentration and disperser-to-extraction solvent ratio set at intermediate levels, was evaluated in four replicates. The subsequent *t*-test yielded a *p*-value of 6.72%, leading to the rejection of the hypothesis that the optimal response lay at the center of the experimental design.

Consequently, the NaCl concentration was systematically increased starting from the central point (0.25 g) across six experimental points (0.30 g, 0.34 g, 0.38 g, 0.42 g, 0.46 g, and 0.50 g), following the steepest ascent method. A second-order polynomial model was fitted to the experimental data collected along the steepest ascent direction to describe the effect of NaCl concentration on the response (Fig. 5).

The model was statistically significant (p-value < 0.001) and showed good predictive ability, explaining 91.6% of the total variance ($R^2 = 0.916$; adjusted $R^2 = 0.892$), with a residual standard error of 0.0073. The local maximum was estimated by the model at a NaCl amount of approximately 0.426 g, which represents the estimated optimum under the investigated experimental conditions.

The response surface modelling was deemed unnecessary as any further mathematical optimization would result in negligible analytical gains compared to the experimental effort.

To quantitatively assess the enhancement in analytical response, the percentage increase in the normalized geometric mean of the chromatographic peak areas for the 12 analytes was calculated. This comparison was performed between the pre-optimization baseline, adopted from the experimental conditions of Bartolini *et al.*,[16] which represents the most recent benchmark in the reviewed literature, and the post-optimization protocol. This yielded a percentage increase of 36%, consistent with the need for a highly sensitive method applicable to valuable figured vases.

Validation

Validation allowed assessment of the method's sensitivity, precision and specificity (Table 4). The absence of detectable peaks confirmed that no carryover occurred during the analytical procedure. Precision was consistently within 15% for all analytes, except for maleic and syringic acids. Regarding linearity, R^2 values exceeded 0.99 for all analytes except palmitic acid ($R^2 = 0.83$) and stearic acid ($R^2 = 0.61$). Consequently, to prevent analytical noise from biasing the PCA clusters, stearic, maleic and syringic acids were excluded from statistical modelling.

Table 4 LOD, precision and linearity of the 12 analytes considered. LOD was defined in ng of analyte per mg of powdered samples

Analyte	LOD (ng mg^{-1})	Precision
Butyric acid	0.0006	9%
Linoleic acid	0.0006	7%
Myristic acid	0.0006	14%
Oleic acid	0.0006	13%
Palmitic acid	0.0006	8%
Stearic acid	0.0006	10%
Fumaric acid	0.0006	2%
Maleic acid	0.0006	24%
Malic acid	0.0114	3%
Syringic acid	0.0571	65%
Succinic acid	0.0006	2%
Tartaric acid	0.5714	6%

Case studies

Venetian blind cross-validation with five groups, employed to determine the optimal number of principal components, indicated that the root mean square error of cross-validation (RMSECV) slightly increases after the addition of each component. Consequently, a simple two-component model was chosen, explaining 72.2% of the total variance while maintaining high interpretability (Fig. 6). A three-component model (90.2% of variance explained) is also presented and discussed in the SI (Fig. S10).

The first principal component (PC1, 44.6% of explained variance) mostly captures the variance distinguishing the milk reference from the other samples. As expected, this separation is driven by the contribution of fatty acids. The only fatty acid increasing along the first principal component is butyric acid.[50] The milk reference sample was noticed to exhibit a progressive attenuation of the butyric acid signal (normalized to the ceramic blank): comparisons between the sample analyzed immediately after artificial ageing and again after six months show that the butyric acid signal declined to levels similar to the baseline. This reduction is consistent with the progressive loss of butyric acid from the milk-enriched ceramic matrix, a documented process for short-chain fatty acids in porous archaeological media.[51]

All analyzed archaeological samples, with the sole exception of 1556, display positive scores along PC1, pointing to an inferior relative abundance of fatty acids in comparison with milk reference. Sample 1556, a red figure askos, represents a unique typology within the analyzed assemblage. Its morphology and small size suggest a potential function as a container for perfumes or anointing oils. Consistent with this hypothesis, its negative score on PC1 reflects a higher relative abundance of fatty acids compared to the other archaeological samples.

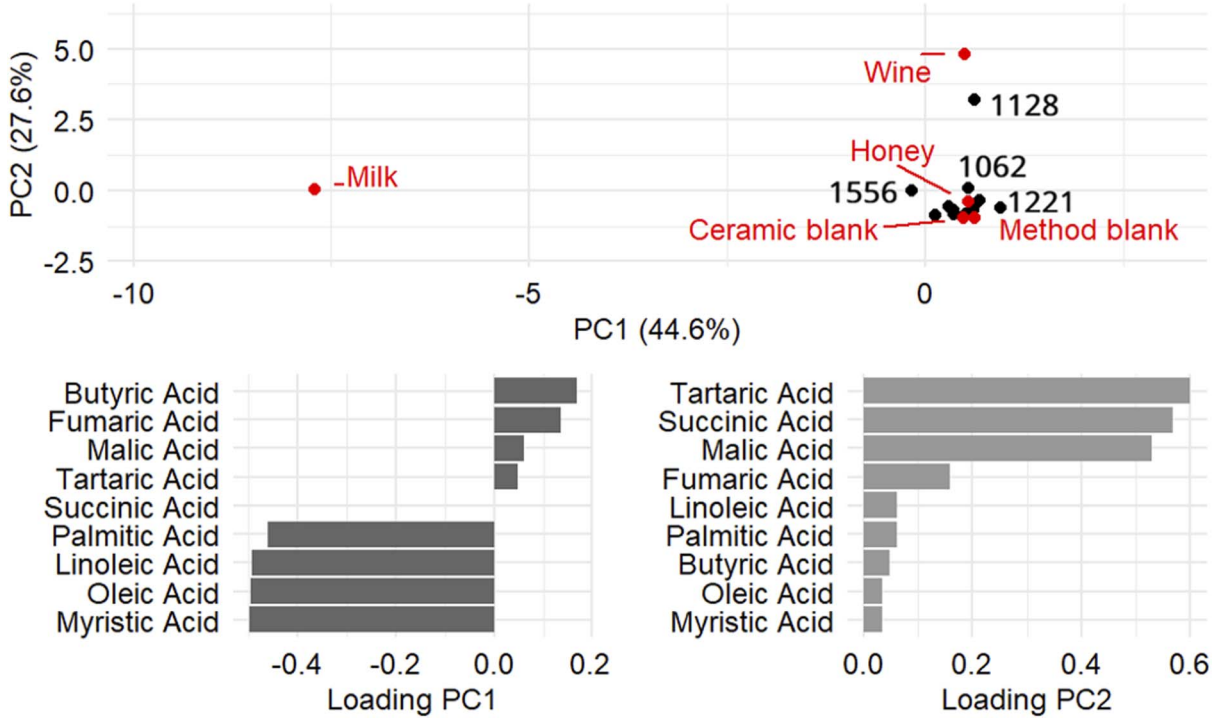

Fig. 6 Principal component analysis performed on the lipid profiles of the Faliscan vases and laboratory reference mock-up samples. (Top) Score plot displaying the first principal component (PC1, accounting for 44.6% of the explained variance) *versus* the second principal component (PC2, accounting for 27.6% of the explained variance). (Bottom) Loading plots illustrating the contribution of the chemical variables (analytes) to the first (Left) and second (Right) principal components, respectively.

However, the proximity between sample 1556 and the other vases suggest that there is no strong chemical affinity with the milk reference, and, due to the low taxonomic specificity of the identified fatty acids, it is currently impossible to ascertain whether the lipid source has animal or plant origin, and further investigation is required.

Conversely, PC2 is positively correlated with short-chain organic acids, especially tartaric, succinic, and malic acids. Indeed, the highest positive score for this component is occupied by wine reference. In this regard, sample 1128 (an overpainted stamnos) stands out for its proximity to the wine reference. Notably, tartaric acid was identified in other vases, too, such as 1062 and 1556. Vases 1128, 1062, and 1156, previously analyzed by Bartolini and coauthors,[16] had already exhibited evidence of tartaric and malic acids, with vases 1062 and 1156 also showing traces of fumaric acid. However, the present study identified tartaric, succinic, and malic acids within the wildflower honey reference as well. This finding aligns with existing literature[52] and corroborates concerns regarding the reliability of tartaric acid alone as a definitive biomarker for wine. The positioning of vases 1556 and 1062 at slightly positive values along PC2 is mainly attributed to their high relative content of malic acid. Despite its higher prevalence in wine compared to honey reference, malic acid lacks the specificity required to serve as a diagnostic biomarker. Therefore, the analytical evidence for wine contact in these vases requires integration with archaeological evidence before robust conclusions can be drawn.

Given its proximity to the wine reference along PC1 and PC2, sample 1128 provides the strongest evidence of contact with wine among the analyzed vases. Notably, Raman spectroscopy also revealed the presence of ash and bone remains in this vase (authors' data, in preparation), supporting its identification as a cinerary urn.

Taken together, these lines of evidence support the hypothesis that wine was used not only as a beverage consumed during banquets but also as a substance of considerable symbolic significance in funerary rituals.

For an enlarged view of the sample cluster in the PC1 and PC2 score plots, including all corresponding vase labels, please refer to the SI (Fig. S11).

Conclusions

In this study, a multivariate approach was employed both to maximize the simultaneous analytical response of 12 fatty acids and wine-related organic acids and to interpret their distribution profiles across archaeological and reference samples. The analytical workflow was specifically developed to support the investigation of ancient use-related residues in Faliscan figured vases from the Museo Archeologico dell'Agro Falisco in Civita Castellana (VT).

From the archaeological perspective, the application of ORA techniques to figured pottery, a material class rarely investigated due to its highly refined ceramics, its limited use, and the constraints imposed by its art-historical value, represents an

 This journal is © The Royal Society of Chemistry 2026

innovation. Developing highly sensitive and robust methodologies tailored to this category can overcome these barriers and open entirely new analytical perspectives.

In this regard, the workflow proved effective using just 35 mg of removed ceramic powder, minimizing damage to objects of artistic and historical values. The experimental design enabled a 36% increase in the analytical response for the targeted analytes compared to the most recent methods. Method validation enabled the selection of the most reliable analytes for data analysis, thereby minimizing the noise introduced into the model.

PCA was performed on 12 archaeological vases and a set of modern reference materials (wine, milk, honey, and a ceramic blank). The reference samples acted as a simplified control model, driving the orientation of the principal components within the PCA space. This renders the relative variance among the target markers highly interpretable, allowing the archaeological samples to be projected and evaluated against known trajectories of the principal axes. In particular, milk, characterized by high abundances of fatty acids, was clearly separated from the wine reference, enriched in low-molecular-weight organic acids, as well as from ceramic blanks. This approach was designed to mitigate the impact of external contaminants and matrix effects, which is inherently challenging to assess in archaeology. While specific interferences can readily distort the signal of an individual compound, the probability of them mimicking the simultaneous response of the entire multi-biomarker suite is statistically negligible.

Regarding results, vase 1128 exhibited a compositional profile more closely resembling wine compared to the other vessels, characterized by the concomitant presence of tartaric, malic, succinic, and fumaric acids. This vase, in which traces of ashes and bone were also detected, corroborates the use of wine not merely as a banquet beverage but also as a highly symbolic substance within funerary contexts.

Overall, this work represents an exploratory step toward the development of more advanced multivariate methodologies. Future efforts should incorporate a broader range of reference samples and analytes to enable the construction of robust classification models. Such models could facilitate the discrimination between different substance classes or, alternatively, support the detection of the presence or absence of residues associated with specific compounds of archaeological relevance, for example, through the application of one-class classification approaches.

Author contributions

AB: conceptualization, methodology, investigation, formal analysis, validation, writing – original draft. MN: investigation, formal analysis. CF: investigation, formal analysis. AP: conceptualization, writing – review and editing. FM: formal analysis, supervision. AC: conceptualization, methodology. GF: supervision. IS: methodology, investigation, supervision, writing – review and editing.

Conflicts of interest

There are no conflicts to declare.

Data availability

Data will be made available on request.

Supplementary information (SI) is available. See DOI: https://doi.org/10.1039/d6ay01076h.

Acknowledgements

The Imag-ORA Project was funded by the European Union – NextGenerationEU – Mission 4 Education and Research – Component 2, Investment 1.2 "Funding of projects submitted by young researchers," project SOE_0000110 "Imag-ORA. Beyond Images in Context. A new interdisciplinary approach for the study of uses and functions of figured pottery in Preroman Italy" CUP F13C22001750001 (PI Dr Angela Pola). A. B. acknowledges support from MUR, PRIN 2022 Project TAMERLANO (grant number 2022427HYH).

References

1 K. J. Brownstein, S. Tushingham, W. J. Damitio, T. Nguyen and D. R. Gang, *Front. Mol. Biosci.*, 2020, **7**, 133.
2 J. Dunne, A. Höhn, G. Franke, K. Neumann, P. Breunig and T. Gillard, *Nat. Commun.*, 2021, **12**, 2227.
3 M. Evans, J. Lundy, A. Lucquin, R. Hagan, Ł. Kowalski, J. Wilczyńki, P. Bickle, K. Adamczak, O. E. Craig, H. K. Robson and J. Hendy, *R. Soc. Open Sci.*, 2023, **10**, 230124.
4 B. Huber, S. Hammann, C. E. Loeben, D. K. Jha, D. G. Vassão, T. Larsen, R. N. Spengler, D. Q. Fuller, P. Roberts, T. Devièse and N. Boivin, *Sci. Rep.*, 2023, **13**, 12477.
5 M. Harano, Y. Date, H. Watanabe and H. Nakata, *Int. J. Hist. Archaeol.*, 2023, **27**, 885–897.
6 L. Lu, R. Wen and J. Cui, *J. Archaeol. Method Theory*, 2024, **31**, 2164–2187.
7 R. Vykukal, A. Gabiger, L. J. Cramp and S. Hammann, *TrAC, Trends Anal. Chem.*, 2024, **176**, 117668.
8 O. E. Craig, J. Lundy, M. Bondetti, S. Nicholson-Lailey, N. Murakami, M. Suzuki, C. Stevens, A. Lucquin, H. M. Talbot, J. Son, S. Fujio, M. Sakamoto, Y. Yamashita, K. Kobayashi, E. R. Crema and S. Shoda, *Proc. Natl. Acad. Sci. U. S. A.*, 2025, **122**(30), e2504414122.
9 N. S. Ramada, M. M. El-Sayed, H. S. Ramadan, M. Ismail, H. Abdelmegeed, N. Gaber and M. M. Sakr, *Food Chem.:Mol. Sci.*, 2025, **11**, 100304.
10 B. Huber, M. Luciani, A. M. Abualhassan, D. Giddings Vassão, R. Fernandes and T. Devièse, *Commun. Biol.*, 2025, **8**, 720.
11 C. A. Dozier, D. Kim and D. H. Russell, *J. Archaeol. Sci. Rep.*, 2020, **32**, 102450.
12 L. d. C. Carvalho, E. Pires, S. Ward, K. Domoney, J. S. O. McCullagh and A. M. Pollard, *J. Archaeol. Sci. Rep.*, 2022, **46**, 103638.

13 L. d. C. Carvalho, E. Pires, K. Domoney, G. Zuchtriegel and J. S. O. McCullagh, *J. Am. Chem. Soc.*, 2025, **147**, 29756–29766.
14 E. Oras, S. Vahur, S. Isaksson, I. Kaljurand and I. Leito, *J. Mass Spectrom.*, 2017, **52**, 689–700.
15 M. Zimmermann, K. J. Brownstein, L. P. Díaz, I. A. Aragón, S. Hutson, B. Kidder, S. Tushingham and D. R. Gang, *Sci. Rep.*, 2021, **11**, 1590.
16 F. Bartolini, F. Vincenti, M. Croce, A. Ciccola, I. Serafini, A. Pola, G. Favero, C. Montesano and M. Sergi, *J. Cult. Herit.*, 2025, **71**, 127–136.
17 F. Vincenti, C. Montesano, P. Babino, S. Carboni, S. Napoletano, G. De Sangro, F. Di Rosa, A. Gregori, R. Curini and M. Sergi, *Forensic Chem.*, 2021, **23**, 100327.
18 B. Huber, T. Larsen, R. N. Spengler and N. Boivin, *Nat. Hum. Behav.*, 2022, **6**, 611–614.
19 J. Lundy, L. Drieu, A. Meo, V. Sacco, L. Arcifa, E. Pezzini, V. Aniceti, G. Fiorentino, M. Alexander, P. Orecchioni, A. Mollinari, M. O. H. Carver and O. E. Craig, *PLoS One*, 2021, **16**(6), e0252225.
20 R. P. Evershed, *Archaeometry*, 2008, **50**, 895–924.
21 A. Irto, G. Micalizzi, C. Bretti, V. Chiaia, L. Mondello and P. Cardiano, *Molecules*, 2022, **27**, 3451.
22 J. La Nasa, F. Modugno and I. Degano, *Mass Spectrom. Rev.*, 2021, **40**, 381–407.
23 L. Drieu, J. Lundy, R. K. Smith, E. Bergström, H. Talbot, M. Primavera, G. Fiorentino, O. E. Craig and J. Thomas-Oates, *Archaeometry*, 2025, **67**, 182–201.
24 L. Drieu, M. Rageot, N. Wales, B. Stern, J. Lundy, M. Zerrer, I. Gaffney, M. Bondetti, C. Spiteri, J. Thomas-Oates and O. E. Craig, *Sci. Technol. Archaeol. Res.*, 2020, **6**(1), 16–29.
25 M. Longoni, M. Lissana, L. Bottaro, F. Malberti, M. Marzullo, D. Teseo, N. Ludwig and S. Bruni, *J. Archaeol. Sci. Rep.*, 2024, **53**, 104365.
26 A. King, T. G. Powis, K. F. Cheong and N. W. Gaikwad, *J. Archaeol. Sci.*, 2017, **85**, 30–40.
27 B. Huber, *Sci. Rep.*, 2026, **16**, 14280.
28 D. Badillo-Sanchez, M. Serrano Ruber, A. M. Davies-Barrett, D. J. Jones and S. Inskip, *J. Archaeol. Sci.*, 2023, **153**, 105769.
29 D. Badillo-Sanchez, M. Serrano Ruber, A. Davies-Barrett, D. J. L. Jones, M. Hansen and S. Inskip, *Sci. Adv.*, 2023, **9**, eadh0485.
30 C. Roullier-Gall, S. S. Heinzmann, J. P. Garcia, P. Schmitt-Kopplin and R. D. Gougeon, *NPJ Sci. Food*, 2017, **1**, 1.
31 E. Dodd and D. Van Limbergen, *Curr. Opin. Food Sci.*, 2025, **64**, 101330.
32 R. G. Brereton, J. Jansen, J. Lopes, F. Marini, A. Pomerantsev, O. Rodionova, J. M. Roger, B. Walczak and R. Tauler, *Anal. Bioanal. Chem.*, 2017, **409**, 5891–5899.
33 E. M. C. Alexandre, P. Araújo, M. F. Duarte, V. de Freitas, M. Pintado and J. A. Saraiva, *Food Bioprocess Technol.*, 2017, **10**, 886–900.
34 M. Magdy, *Microchem. J.*, 2025, **217**, 115023.
35 M. Correa-Ascencio and R. P. Evershed, *Anal. Methods*, 2014, **6**, 1330–1340.
36 M. Regert, *Mass Spectrom. Rev.*, 2011, **30**, 177–220.
37 J. J. Lucejko, J. La Nasa, F. Porta, A. Vanzetti, G. Tanda, C. F. Mangiaracina, A. Corretti, M. P. Colombini and E. Ribechini, *Sci. Rep.*, 2018, **8**, 3935.
38 L. Blanco-Zubiaguirre, E. Ribechini, I. Degano, J. La Nasa, J. A. Carrero, J. Iñañez, M. Olivares and K. Castroa, *Microchem. J.*, 2018, **137**, 190–203.
39 J. Han, K. Lin, C. Sequria, J. Yang and C. H. Borchers, *Electrophoresis*, 2016, **37**, 1851–1860.
40 G. Liebisch, J. Ecker, S. Roth, S. Schweizer, V. Öttl, H. F. Schött, H. Yoon, D. Haller, E. Holler, R. Burkhardt and S. Matysik, *Biomolecules*, 2019, **9**, 121.
41 C. D'Addario, M. Pucci, F. Bellia, A. Girella, A. Sabatucci, F. Fanti, M. Vismara, B. Benatti, L. Ferrara, F. Fasciana, L. Celebre, C. Viganò, L. Elli, M. Sergi, M. Maccarrone, V. Buzzelli, V. Trezza and B. Dell'Osso, *Clin. Epigenet.*, 2022, **14**, 47.
42 P. Viñas, N. Campillo, I. López-García and M. Hernández-Córdoba, *Anal. Bioanal. Chem.*, 2014, **406**, 2067–2099.
43 F. F. F. Vincenti, C. Montesano, M. Serafini, D. Compagnone and M. Sergi, *J. Pharm. Biomed. Anal.*, 2020, **186**, 113302.
44 F. Vincenti, C. Montesano, L. Celluccia, A. Gregori, F. Fanti, D. Compagnone, R. Curini and M. Sergi, *J. Chromatogr. A*, 2019, **1605**, 360348.
45 A. Bosi, A. Ciccola, I. Serafini, S. Berbers, A. N. P. Gaibor, E. Cwiertnia, P. Postorino, G. Favero and M. R. van Bommel, *Talanta*, 2025, **293**, 128041.
46 A. Bosi, A. Ciccola, I. Serafini, G. Peruzzi, V. Nigro, P. Postorino, R. Curini and G. Favero, *Molecules*, 2023, **28**, 108447.
47 F. Vincenti, C. Montesano, A. Ciccola, I. Serafini, G. Favero, M. Pallotta, F. Pagano, G. Di Francesco, M. Croce, M. L. Leone, I. M. Muntoni and M. Sergi, *Front. Chem.*, 2023, **11**, 1238793.
48 A. Cozza and A. Pasqui, *Carta archeologica d'Italia (1881–1897): materiali per l'agro falisco*, L.S. Olschki, 1981.
49 A. Pola, *La più antica produzione ceramica falisca a figure rosse*, Giorgio Bretschneider Editore, 2024.
50 D. Steiner, R. Krska, A. Malachová, I. Taschl and M. Sulyok, *J. Agric. Food Chem.*, 2020, **68**, 3868–3880.
51 M. S. Copley, R. Berstan, S. N. Dudd, G. Docherty, A. J. Mukherjee, V. Straker, S. Payne and R. P. Evershed, *Proc. Natl. Acad. Sci. U. S. A.*, 2003, **100**, 1524–1529.
52 L. Sun, F. Shi, X. He, Y. Cai, Y. Yu, D. Yao, J. Zhou and X. Wei, *Eur. Food Res. Technol.*, 2023, **249**, 473–484.

 This journal is © The Royal Society of Chemistry 2026